

# Doxorubicin–NO Releaser Molecular Hybrid Activatable by Green Light to Overcome Resistance in Breast Cancer Cells

Cristina Parisi,<sup>†</sup> Francesca Moret,<sup>†</sup> Aurore Fraix, Luca Menilli, Mariacristina Failla, Federica Sodano, Claudia Conte, Fabiana Quaglia, Elena Reddi, and Salvatore Sortino\*



Cite This: *ACS Omega* 2022, 7, 7452–7459



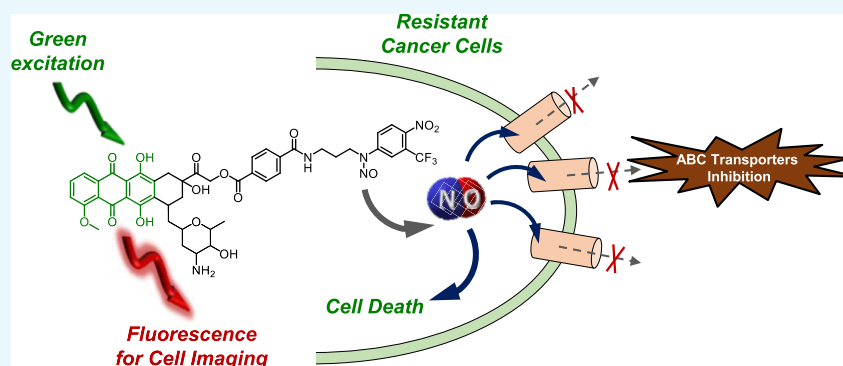
Read Online

ACCESS |

Metrics & More

Article Recommendations

Supporting Information



**ABSTRACT:** The biological activity of a molecular hybrid (DXNO-GR) joining doxorubicin (DOX) and an N-nitroso moiety releasing nitric oxide (NO) under irradiation with the biocompatible green light has been investigated against DOX-sensitive (MCF7) and -resistant (MDA-MB-231) breast cancer cells *in vitro*. DXNO-GR shows significantly higher cellular internalization than DOX in both cell lines and, in contrast to DOX, does not experience cell efflux in MDR overexpressing MDA-MB-231 cells. The higher cellular internalization of the DXNO-GR hybrid seems to be mediated by bovine serum albumin (BSA) as a suitable carrier among serum proteins, according to the high binding constant measured for DXNO-GR, which is more than one order of magnitude larger than that reported for DOX. Despite the higher cellular accumulation, DXNO-GR is not toxic in the dark but induces remarkable cell death following photoactivation with green light. This lack of dark toxicity is strictly related to the different cellular compartmentalization of the molecular hybrid that, different from DOX, does not localize in the nucleus but is mainly confined in the Golgi apparatus and endoplasmic reticulum and therefore does not act as a DNA intercalator. The photochemical properties of the hybrid are not affected by binding to BSA as demonstrated by the direct detection of NO photorelease, suggesting that the reduction of cell viability observed under light irradiation is a combined effect of DOX phototoxicity and NO release which, ultimately, inhibits MDR1 efflux pump in DOX-resistant cells.

## INTRODUCTION

The development of molecular hybrids in which two pharmacologically active entities are covalently joined in the same molecular skeleton is emerging as an area with great expansion for potential development of novel therapeutic strategies.<sup>1–3</sup> These molecular constructs represent a powerful tool for the discovery of new drugs for treating important diseases as cancer. In fact, hybrid drugs offer the possibility for combination therapies achieved with a single multifunctional “super molecule” that, in principle, is expected to be more specific and powerful than conventional drugs.<sup>1–3</sup>

Doxorubicin (DOX) is one of the most widely employed chemotherapeutics for treating a variety of solid tumors, including breast, ovarian, bladder, and lung tumors.<sup>4</sup> However, the high and dose-limiting cardiotoxicity, associated to the development of resistance, hampers the clinical use of this

anthracycline derivative.<sup>5</sup> Among the several mechanisms at the basis of multidrug resistance (MDR), for DOX, this phenomenon seems to be closely related to an increased efflux of the drug from tumor cells as a result of the overexpression of ATP binding cassette (ABC) transporters (e.g., efflux pumps).<sup>6–8</sup> Therefore, co-administration of DOX with compounds able to hamper ABC transporters functionality and consequently block drug extrusion has been proposed as valuable approach to overcome resistance.<sup>9</sup> Nevertheless, this

Received: July 26, 2021

Accepted: November 24, 2021

Published: February 24, 2022

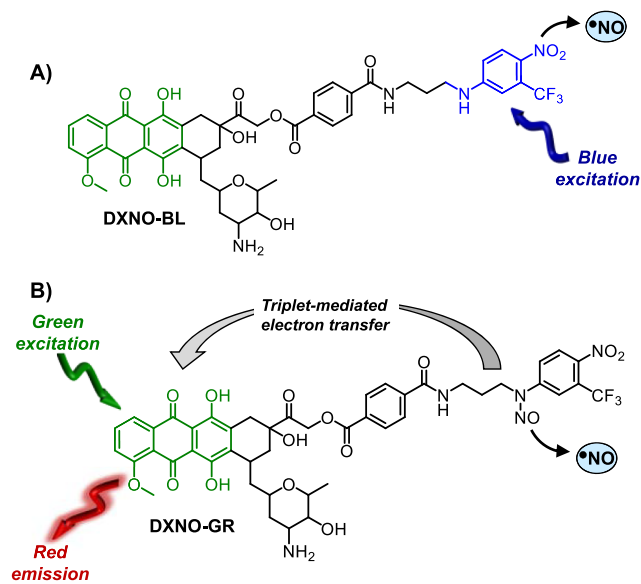


strategy suffers from a number of pharmacokinetic and pharmacodynamic limitations.<sup>10</sup>

Nitric oxide (NO) is a small, inorganic free radical that, besides being a well-known bioregulator of vital functions in the human body, plays a key role in tumour biology.<sup>11</sup> In this regard, the effects of NO are strictly depending on its doses.<sup>12</sup> Concentrations in the pM–nM range encourage tumour progression,<sup>13</sup> whereas higher concentrations, in the  $\mu\text{M}$  range, promote apoptosis through nitration of crucial mitochondrial enzymes,<sup>14,15</sup> or *via* oxidative and nitrative stress.<sup>16</sup> Moreover,  $\mu\text{M}$  concentrations of NO inhibit the cellular extrusion of DOX in human cancer cells mainly through a mechanism involving nitration of critical tyrosine residues of MDR1 (P-gp), ABCB1, and MRPs/ABCCs transporters.<sup>17,18</sup> On these bases, molecular hybrids in which DOX is covalently linked to NO-releasing moieties have been synthesized and proven to induce considerable ABC transporters inhibition.<sup>19–21</sup> However, these compounds lack spatiotemporal control of NO release and require high concentrations of the NO donors and long incubation time to obtain an intracellular NO level sufficient for protein nitration.

For such reasons, light activatable NO donors, namely, NO photodonors (NOPDs), are much more appealing than NO precursors liberating spontaneously NO.<sup>22–25</sup> In fact, light triggering allows for NO dosage to be precisely controlled by tuning the time and the intensity of irradiation. At this regard, we have reported the first molecular hybrid of DOX with a NOPD, DXNO-BL (Scheme 1A), able to release NO upon

**Scheme 1. Structures of the Molecular Hybrid DXNO-BL (A) and DXNO-GR (B) Releasing NO under Blue and Green Light Excitation, Respectively**



irradiation with blue light, to inhibit efflux pumps responsible for DOX resistance and to induce significant cancer cells mortality.<sup>26</sup> Very recently, we have demonstrated that the nitroso derivative of DXNO-BL, the hybrid DXNO-GR (Scheme 1B) permits NO uncaging with the much more biocompatible and tissue penetrating green light, representing an advantage of more than 100 nm in terms of excitation wavelength.<sup>27</sup> As recalled in Scheme 1B for sake of clarity, in this case the DOX component acts as green light harvesting

antenna and triggers NO release from the N-nitroso appendage *via* a triplet-state mediated intramolecular electron transfer, without precluding the typical red emission useful for cellular tracking of the hybrid. Moreover, DXNO-GR binds isolated DNA *in vitro* with a binding constant higher than that of the free DOX, preserving the NO photoreleasing property, even in the bounded form.<sup>27</sup> On these premises, to gain insights into the potential photo-chemotherapeutic properties of this molecular hybrid and the related mechanisms of action, we investigated *in vitro* its behaviour on different breast cancer cells using free DOX as reference compound.

## RESULTS AND DISCUSSION

Adenocarcinoma MCF7 and MDA-MB-231 triple negative breast cancer cells were categorized as MDR1-negative and MDR1-positive, respectively, on the basis of their expression of MDR1 pump (Table S1) evaluated by flow cytometry analyses and expressed as MDR activity factor (MAF). Indeed, MDA-MB-231 showed over-expression of MDR1 pump, having a MAF of 54 versus MAF in MCF7 approx. equal to zero. Of note, both cell lines can be considered positive for the expression of MRP1/2, while they showed minor expression of BCRP (Table S1), even if, in any case, the major player in inducing DOX resistance in breast cancer is reported to be the MDR1 pump.<sup>28</sup>

Cytotoxicity of DXNO-GR and, for sake of comparison, of DOX was evaluated in MCF7 and MDA-MB-231 cancer cells incubated for 2 h with increasing concentration of drugs (0–10  $\mu\text{M}$ ) in the absence of irradiation (dark cytotoxicity) or exposing cells to green light (photo-toxicity; total dose 72 J/cm<sup>2</sup>) at the end of the incubation time. Cell viability was measured with the MTS assay after 24 h incubation in a drug-free medium (Figure 1).

Dark cytotoxicity experiments (Figure 1a,c) showed that DXNO-GR does not induce any significant reduction of cell viability in both cell lines, in contrast to DOX, that is highly cytotoxic towards MCF7 cells (IC<sub>50</sub> DOX 7.6  $\mu\text{M}$ ). Therefore, based on the latter results, MDA-MB-231 and MCF7 can be considered as DOX-resistant and DOX-sensitive, respectively, in accordance with their MDR1 expression. Irradiation with green light (Figure 1b,d) leads to a different scenario with DXNO-GR exhibiting significant cytotoxic action towards both cell lines (IC<sub>50</sub> is 3.9 and 0.46  $\mu\text{M}$  for MDA-MB-231 and MCF7, respectively). Although in a lesser extent than the hybrid, a photodynamic effect is also observed for DOX, with the difference between the two compounds being much more pronounced in the case of resistant MDA-MB-231 cells.

To gain insights into the mechanism of action of the molecular hybrid, we first evaluated its cellular uptake by flow cytometry analysis, after different incubation times, exploiting DOX fluorescence. Figure 2a clearly shows that the cellular accumulation of DXNO-GR in both cell lines is more than 5-fold higher than that observed for DOX.

Interestingly, the cellular uptake of DXNO-GR was not affected by verapamil treatment, a typical inhibitor of the MDR1 efflux pump, in both cell lines, while, as expected, verapamil significantly increased the intracellular uptake of DOX exclusively in MDR1 over-expressing MDA-MB-231 cells. Therefore, this result underlines that the hybrid DXNO-GR does not suffer of cell extrusion through a MDR1-mediated mechanism (Figure 2b).

Considering our previous finding on more effective intercalation of DXNO-GR with respect to DOX to isolated

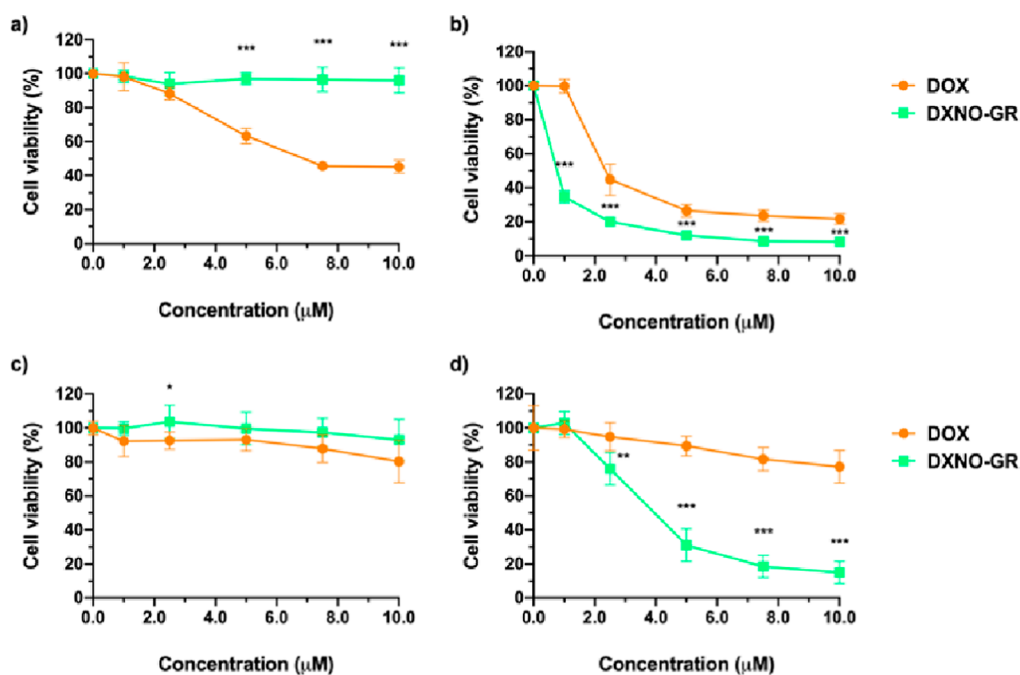


**Figure 1.** Decrease of viability in MCF7 (a,b) and MDA-MB-231 (c,d) breast cancer cells after incubation for 2 h with increasing concentrations of DXNO-GR or DOX in the dark (a,c) or after green light irradiation ( $72 \text{ J/cm}^2$ ) (b,d). Cells were incubated for 24 h before assessing cell viability. Data are expressed as mean percentage  $\pm$  SD of at least three independent experiments, carried out in triplicate. \* $p < 0.05$ ; \*\* $p < 0.01$ ; \*\*\* $p < 0.001$  significantly different from DOX (Student's *t*-test).

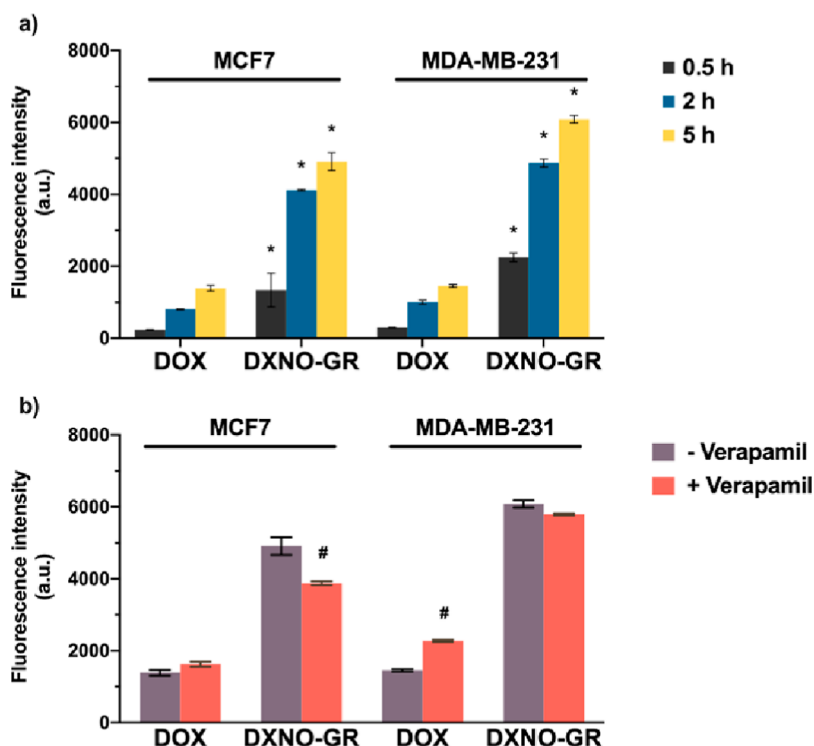


**Figure 2.** Cellular uptake of  $2.5 \mu\text{M}$  DOX and DXNO-GR in MCF7 and MDA-MB-231 cells measured by flow cytometry in the absence (a) or in the presence (b) of the MDR-1 inhibitor verapamil ( $50 \mu\text{M}$ ). Data are expressed as mean fluorescence intensity (a.u.)  $\pm$  SD of at least three independent experiments, carried out in triplicate. \* $p < 0.001$  significantly different from DOX (Student's *t*-test); # $p < 0.001$  significantly different from verapamil (Student's *t*-test).

DNA *in vitro*,<sup>27</sup> the lack of dark cytotoxicity of the molecular hybrid in MCF7 cells (Figure 1a), appears quite surprising and clearly suggests that the anticancer activity of DOX is not preserved after its covalent conjugation to the NOPD moiety.

Confocal microscopy analysis allowed explaining this discrepancy. The images of Figure 3 provide clear-cut evidence that, in contrast to DOX (Figure S1), the hybrid DXNO-GR does not localize in the nucleus of MDA-MB-231 cells, neither after a 2

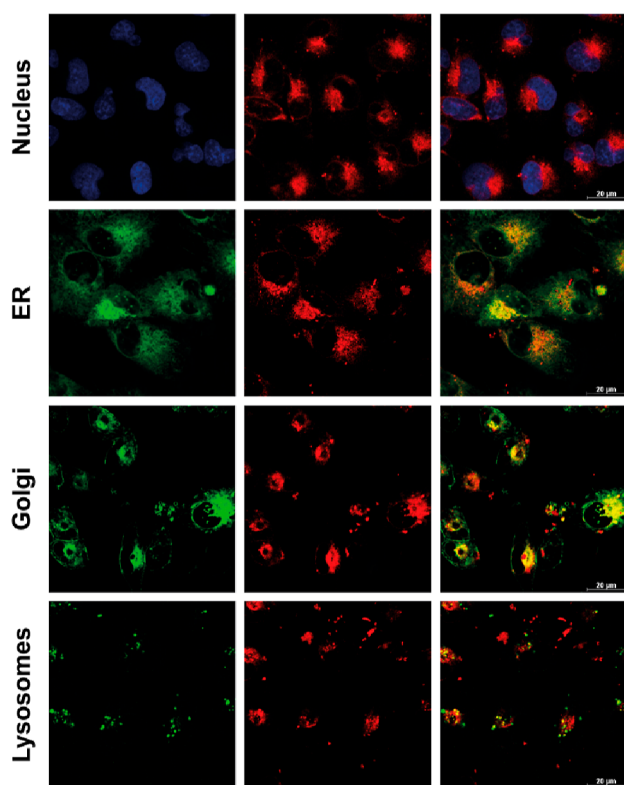


**Figure 3.** Intracellular localization of DXNO-GR in MDA-MB-231 cells after 2 h of incubation. Confocal microscopy images show the absence of co-localization between DXNO-GR (red fluorescence) and the nucleus (stained with Hoechst-33342). DXNO-GR fluorescence clearly co-localized with endoplasmic reticulum (ER-Tracker Green probe) and Golgi apparatus (BODIPY FL C5-ceramide probe).

h incubation neither after 16 h (Figure S2). Indeed, DXNO-GR mainly localizes in the Golgi apparatus and in the endoplasmic reticulum (Figure 3), thus precluding any DNA intercalation and, as a consequence, any cytotoxic activity operating by mechanisms similar to those of DOX. Of note, our confocal microscopy analysis showed that for long incubation times (e.g., 16 h, Figure S2) DXNO-GR localized exclusively in the Golgi apparatus. In any case, the higher cellular uptake of DXNO-GR with respect to DOX cannot be simply explained with the lack of cellular extrusion by the ABC transporters. In fact, the hybrid internalized more efficiently than DOX also in the MDR-1 negative MCF7 cells.

Uptake of DOX in resistant and non-resistant cells is a complex phenomenon governed by its chemical–physical properties (ionization and lipophilicity) and plasma membrane composition besides drug efflux mechanisms.

DXNO-GR has a  $pK_a$  comparable to DOX (ca 8.5) and thus ionization degree is not expected to affect the overall lipophilicity at physiological pH. The experimental value of the partition coefficient between *n*-octanol and PBS at pH 7.4 for DXNO-GR was higher than that of DOX ( $\log D_{7.4}$  of  $-0.04$  and  $-0.87$  for DXNO-GR and DOX, respectively). This increase in lipophilicity explains the superior uptake of DXNO-GR into both cell lines, and is consistent with the evidence that the permeability of cells to the anthracyclines is mediated via the lipid domain of the plasma membrane as shown for DOX.<sup>29</sup>

To gain more insights into the mechanisms of DXNO-GR uptake, we investigated if internalization mechanisms other than passive diffusion were exploited by cells for hybrid internalization. Accordingly, we found that the accumulation of drugs in both cell lines was largely depressed at 4 °C (Figure S3), suggesting that the uptake of DXNO-GR, but also that of DOX, occurred through energy-dependent mechanisms other than simple diffusion through plasma membranes. Therefore, we turned at bovine serum albumin (BSA) as a possible player in the internalization process, on the basis of evidence demonstrating that it can facilitate the transport of drugs inside cancer cells through endocytic pathways.<sup>30</sup> Furthermore, because albumin is present in the culture medium as the prevailing serum component (e.g., in our *in vitro* experimental conditions serum accounts for the 10% of the culture medium), it must be considered that its binding with the tested anticancer drugs can profoundly affect internalization extents and the cytotoxic effects.

The binding properties of DXNO-GR with BSA were studied by means of steady-state and time-resolved fluorescence techniques.

The analysis of the fluorescence of BSA in the presence of increasing amounts of drug is usually the most suited approach to obtain the binding properties of the protein with a specific guest. When excited at 280 nm BSA shows an emission band with maximum at ca. 340 nm due to the tryptophan residue. Addition of increasing concentration of DXNO-GR considerably quenches this emission, accounting for an interaction between the two components (Figure 4). Moreover, the slight

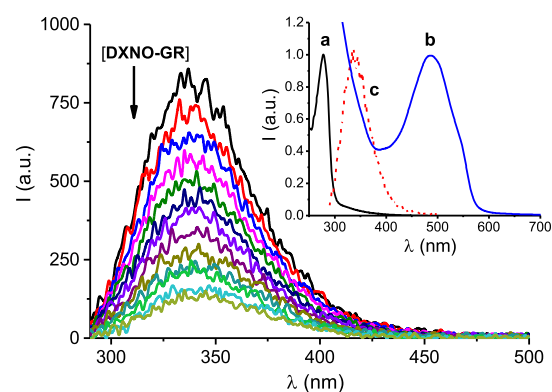


**Figure 4.** Fluorescence emission spectra ( $\lambda_{\text{exc}} = 280$  nm) of BSA (10  $\mu\text{M}$ ) observed upon addition of increasing amount of DXNO-GR from 0 to 80  $\mu\text{M}$ . The inset shows the normalized absorption spectra of BSA (a) and DXNO-GR (b) and the fluorescence emission spectrum of BSA (c).  $T = 25$  °C, pH 7.4.

red shift of the fluorescence maximum observed upon addition of the hybrid reveals that the tryptophan fluorophore experiences a more hydrophilic environment due to the BSA/DXNO-GR interaction.

Note that the absorption of DXNO-GR at the excitation wavelength of BSA and the overlap of the emission of BSA with the absorption of DXNO-GR (see inset of Figure 4, for sake of clarity) make necessary all the spectra of Figure 4 to be corrected according to eq 1<sup>31</sup>

$$F_c = F_m e^{(A_1 + A_2)/2} \quad (1)$$

where  $F_c$  and  $F_m$  are the corrected and measured fluorescence, respectively, and  $A_1$  and  $A_2$  are the absorbance values of

DXNO-GR at the excitation and emission wavelength, respectively. Such correction is necessary in order to eliminate a trivial fluorescence decrease arising from an inner filter effect due to competitive absorption of the excitation light and re-absorption of the emitted light.

In order to establish the nature of the quenching mechanism, static or dynamic, we plotted the fluorescence data according to the Stern–Volmer eq 2<sup>32</sup>

$$I_0/I = 1 + K_{SV}[\text{DXNO-GR}] \quad (2)$$

where  $I_0$  and  $I$  are the intensity fluorescence in the absence and in the presence of the hybrid, respectively and  $K_{SV}$  (Stern–Volmer constant) =  $k_q\tau$ , with  $k_q$  and  $\tau$  being the bimolecular quenching constant and the lifetime of the fluorophore in the absence of the hybrid, respectively. From the linear part of the plot reported in Figure 5A we obtained a value for  $K_{SV} = 1.95$

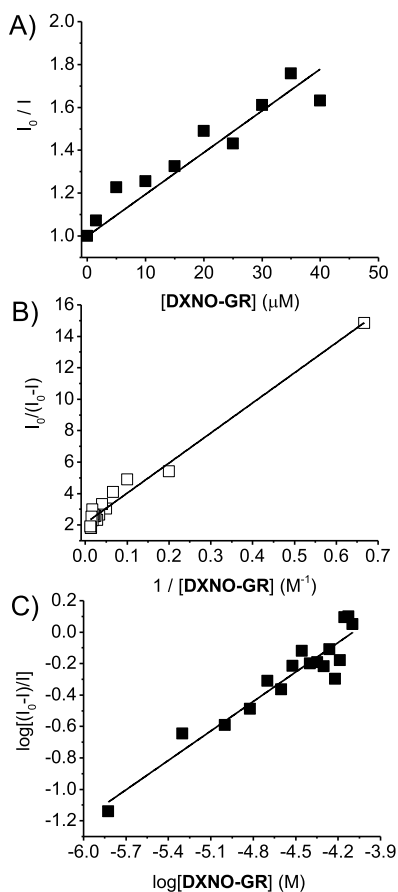


**Figure 5.** Plots of the data of Figure 4, corrected by eq 1, according to eq 2 (A), (3) (B) and (4) (C).  $T = 25\text{ }^\circ\text{C}$ , pH 7.4.

$\times 10^4\text{ M}^{-1}$ . Since the average value for  $\tau = 5.9\text{ ns}$ ,  $k_q$  results to be  $3.3 \times 10^{12}\text{ M}^{-1}\text{ s}^{-1}$ . This value exceeds by more than 2 order of magnitude the diffusional rate constant, suggesting that the quenching process takes place exclusively through a static mechanism according to the formation of a non-fluorescent BSA/DXNO-GR complex.

The binding constant  $K_b$  and the fraction of fluorophore accessible to quencher,  $f$ , where obtained by the modified Stern–Volmer eq 3<sup>32,33</sup>

$$I_0/(I_0 - I) = 1/(fK_b[\text{DXNO-GR}]) + 1/f \quad (3)$$

From the data of the plot reported in Figure 5B, we obtained  $K_b = 1.05(\pm 0.07) \times 10^5\text{ M}^{-1}$  and  $f = 0.50 \pm 0.05$ . Furthermore, the number  $n$  of hybrid molecules bound/BSA molecule, resulted  $0.62 \pm 0.05$ , obtained by the plot of Figure 5C and according to eq 4<sup>34</sup>

$$\log[(I_0 - I)/I] = \log K_b + n \log[\text{DXNO-GR}] \quad (4)$$

Note that the value of  $K_b$  obtained is more than one order of magnitude larger than that reported for DOX under identical experimental conditions ( $K_b = 7.8 (\pm 0.7) \times 10^3\text{ M}^{-1}$ ).<sup>35</sup> This result is in excellent agreement with the higher cellular internalization found for the hybrid and suggests that BSA can play a key role as a carrier in this process.

In light of this effective binding with the protein, we consider indispensable to verify that the photophysical and photochemical properties of DXNO-GR are preserved even in its BSA-bounded form. This is not trivial because the confinement of photoactivatable guests in specific compartments of a host can lead to dramatic changes of the photo-reactivity, in nature, efficiency of both, due to steric constrains, specific interaction and polarity effects. Fluorescence dynamic and NO photo-release capability of DXNO-GR were investigated in the presence of BSA under conditions of almost 100% complexation by using time-resolved fluorescence and an ultrasensitive NO electrode, respectively. Figure 6A

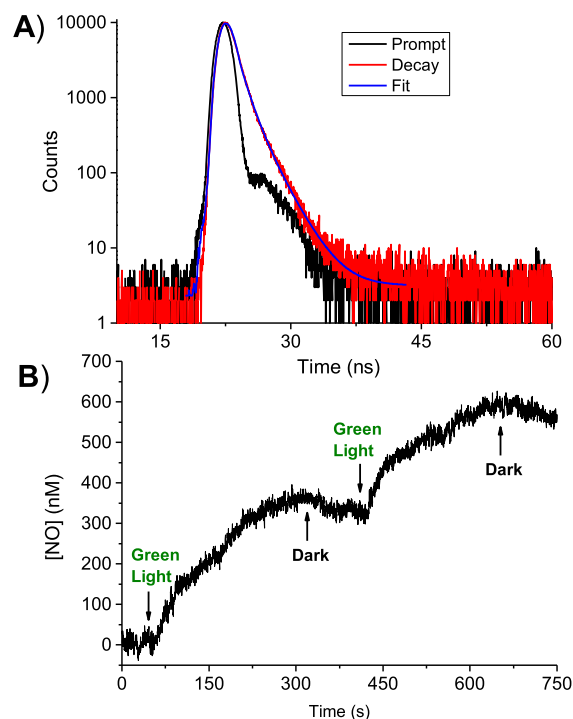


**Figure 6.** (A) Fluorescence decay and the related fitting of the DXNO-GR recorded at  $\lambda_{exc} = 455\text{ nm}$  and  $\lambda_{em} = 600\text{ nm}$ . (B) NO release profile observed for a solution of DXNO-GR in the presence of BSA upon alternate cycles of green light ( $\lambda_{exc} = 532\text{ nm}$ ) and dark.  $[\text{BSA}] = 10\text{ mM}$ ;  $[\text{DXNO-GR}] = 80\text{ }\mu\text{M}$ .  $T = 25\text{ }^\circ\text{C}$ , pH 7.4.

shows that the fluorescence decay of the molecular hybrid exhibits a biexponential behavior with lifetimes  $\tau_1 = 0.82\text{ ns}$  and  $\tau_2 = 1.97\text{ ns}$  with relative amplitudes  $A_1 = 76\%$  and  $A_2 = 24\%$ , respectively. These values are very similar with respect to those observed in the same solvent in the absence of BSA ( $\tau_1 = 1.01\text{ ns}$  and  $\tau_2 = 2.40\text{ ns}$  with relative amplitudes  $A_1 = 85\%$  and

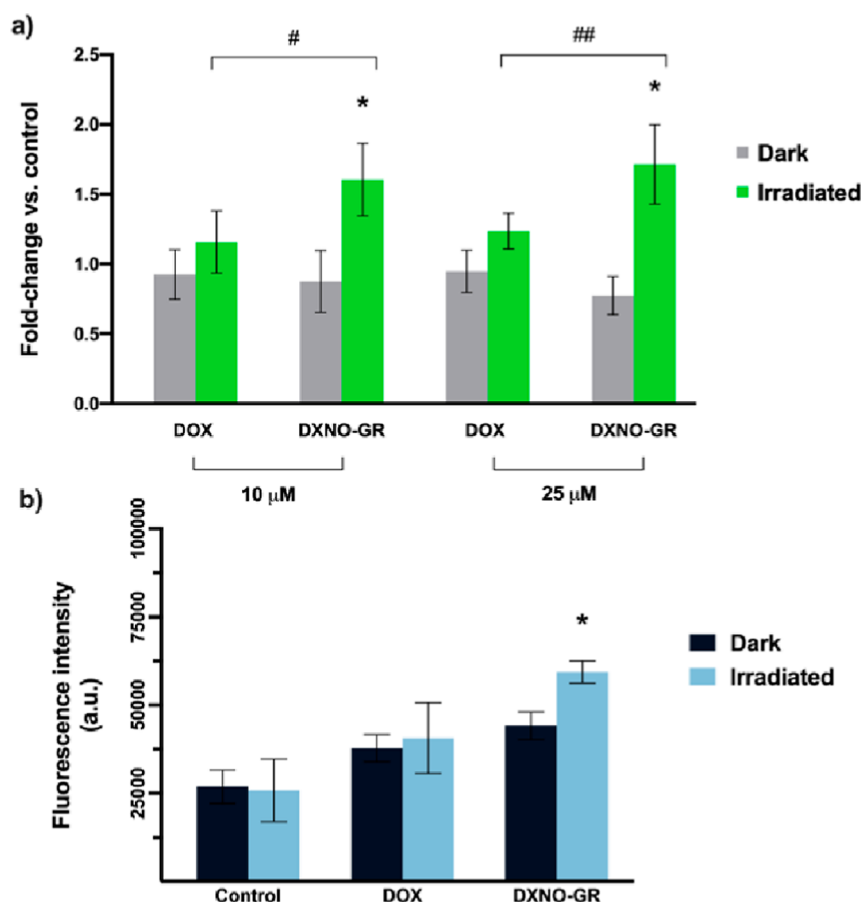


**Figure 7.** (a) Detection of the intracellular levels of NO generated by DXNO-GR or DOX in the absence or in the presence of green light irradiation. NO increment is expressed as increase of DAF-FM probe fluorescence with respect to the fluorescence signal measured in control cells and set equal to 1 (*fold change*). \* $p < 0.001$  significantly different from dark sample (Student's *t*-test). # $p < 0.01$ ; ## $p < 0.001$  significant difference between DOX and DXNO-GR (Student's *t*-test). (b) Inhibition of MDR efflux pumps measured through the retention of the substrate EFLUXX-ID. \* $p < 0.001$  significantly different from dark sample (Student's *t*-test).

$A_2 = 15\%$ , respectively), suggesting that the excited singlet state of DXNO-GR is only slightly affected by the protein binding. Figure 6B shows that, analogously to what already observed for the free hybrid, NO release from the BSA/DXNO-GR complex occurs exclusively upon excitation with green light stimuli, stops in the dark, and restart as the light is switched on again. Because the NO photo-release is mediated by the lowest excited triplet state,<sup>27</sup> our findings demonstrated that also this excited state is not involved in any competitive reaction with protein components.

Intracellular photo-generation of NO from DXNO-GR was measured by flow cytometry using the probe DAF-FM, which becomes fluorescent after NO binding. As illustrated in Figure 7a, the incubation of MDA-MB-231 cells with DXNO-GR did not elicit any significant increase of the intracellular NO level in the dark (fluorescence fold change ca. 1). On the contrary, in cells exposed to light after incubation with DXNO-GR, DAF-FM fluorescence exhibited at least a two-fold increase with respect to cells not exposed to light. In cells incubated with DOX, DAF-FM fluorescence was only slightly increased after irradiation, very likely for an upregulation of inducible NO synthase.<sup>17,18</sup> Intracellular NO generation mediated by the green light has also an inhibitory effect on the efflux pumps (Figure 7b) as found for the blue light activatable DXNO-BL molecular hybrid.<sup>26</sup> In fact, in MDA-MB-231 cells, we observed that the intracellular accumulation of a MDR-pump

substrate (e.g. EFLUXX-ID) significantly increased exclusively in cells incubated with DXNO-GR and exposed to light, indicating the direct inhibition of the pumps upon NO photo-release.

Note that premised that the exclusive activation of DXNO-GR directly at the tumor site by means of locally delivered green light represents the main strategy to promote exclusive phototoxicity and NO generation in malignant cells, in order to counteract off-target effects in normal cells, for sake of comparison, we studied hybrid behaviors also in non-tumorigenic breast MCF-10A cells (Figure S4). Importantly, even if the extent of DXNO-GR uptake was comparable with those measured in the malignant cell lines, dark cytotoxicity was limited (e.g. maximum of 20% viability reduction at the higher dose tested) and reduced with respect of that of DOX (Figure S4a,c). As expected, when DXNO-GR was activated by light, significant NO release (Figure S4d) and cell viability reduction were observed, being in any case DXNO-GR IC50 (1.85  $\mu\text{M}$ ) higher than that measured in cancerous MCF-7 cells (0.46  $\mu\text{M}$ ).

## CONCLUSIONS

This study has provided important insights into the mechanism of action of the DOX-based molecular hybrid DXNO-GR releasing NO under the control of green light. Despite its binding capability to isolated DNA and cellular internalization

are higher than those of DOX, and it does not suffer cell extrusion by MDR-pumps, DXNO-GR does not show any cytotoxic action in the absence of light exposure neither towards DOX-sensitive and -resistant cancer cells nor toward non-malignant breast epithelial cells. This is due its retention mainly in the Golgi apparatus and endoplasmic reticulum, which precludes inhibition of topoisomerase II upon intercalation into DNA at nuclear level similarly to DOX. The hybrid binds BSA with a binding constant higher than that reported for DOX, and this effective protein binding seems to have a role in its efficient intracellular internalization. In addition, protein binding does not affect the NO photo-releasing properties of the molecular hybrid, which produces NO under green light even when bound to BSA and, even more importantly at the intracellular level. The photogenerated NO seems to be the dominant species responsible for the remarkable level of toxicity observed under light irradiation on both types of cell lines and for the inhibition of the efflux pumps in MDA-MB-231 DOX-resistant cells.

## ■ ASSOCIATED CONTENT

### SI Supporting Information

The Supporting Information is available free of charge at <https://pubs.acs.org/doi/10.1021/acsomega.1c03988>.

Materials and instrumentation; lipophilicity of the compounds; binding studies with BSA; cells; dark and photo-toxicity; intracellular uptake studies; intracellular localization studies; intracellular quantification of NO; MDR1 inhibition by DXNO-GR; and statistical analysis (PDF)

## ■ AUTHOR INFORMATION

### Corresponding Author

Salvatore Sortino – Department of Drug and Health Sciences, University of Catania, I-95125 Catania, Italy; [orcid.org/0000-0002-2086-1276](https://orcid.org/0000-0002-2086-1276); Email: [ssortino@unict.it](mailto:ssortino@unict.it)

### Authors

Cristina Parisi – Department of Drug and Health Sciences, University of Catania, I-95125 Catania, Italy  
Francesca Moret – Department of Biology, University of Padova, I-35131 Padova, Italy; [orcid.org/0000-0002-1534-3714](https://orcid.org/0000-0002-1534-3714)  
Aurore Fraix – Department of Drug and Health Sciences, University of Catania, I-95125 Catania, Italy  
Luca Menilli – Department of Biology, University of Padova, I-35131 Padova, Italy; [orcid.org/0000-0003-2774-6411](https://orcid.org/0000-0003-2774-6411)  
Mariacristina Failla – Department of Science and Drug Technology, University of Torino, I-10125 Torino, Italy  
Federica Sodano – Department of Drug and Health Sciences, University of Catania, I-95125 Catania, Italy; Department of Science and Drug Technology, University of Torino, I-10125 Torino, Italy; [orcid.org/0000-0003-2013-4893](https://orcid.org/0000-0003-2013-4893)  
Claudia Conte – Drug Delivery Laboratory, Department of Pharmacy, University of Napoli Federico II, I-80131 Napoli, Italy  
Fabiana Quaglia – Drug Delivery Laboratory, Department of Pharmacy, University of Napoli Federico II, I-80131 Napoli, Italy; [orcid.org/0000-0001-6223-0782](https://orcid.org/0000-0001-6223-0782)  
Elena Reddi – Department of Biology, University of Padova, I-35131 Padova, Italy

Complete contact information is available at:

<https://pubs.acs.org/10.1021/acsomega.1c03988>

## Author Contributions

<sup>†</sup>C.P. and F.M. equally contributed.

## Notes

The authors declare no competing financial interest.

## ■ ACKNOWLEDGMENTS

We thank AIRC—Italian Association for Cancer Research (IG-19859) for financial support.

## ■ REFERENCES

- (1) Meunier, B. Hybrid molecules with a dual mode of action: Dream or Reality. *Acc. Chem. Res.* **2008**, *41*, 69–77.
- (2) *Design of Hybrid Molecules for Drug Development*, 1st ed.; Decker, M., Ed.; Elsevier, 2017.
- (3) Bérubé, G. An overview of molecular hybrids in drug discovery. *Expert Opin. Drug Discov.* **2016**, *11*, 281–305.
- (4) Minotti, G.; Menna, P.; Salvatorelli, E.; Cairo, G.; Gianni, L. Anthracyclines: molecular advances and pharmacologic developments in antitumor activity and cardiotoxicity. *Pharmacol. Rev.* **2004**, *56*, 185–229.
- (5) Swain, S. M.; Whaley, F. S.; Ewer, M. S. Congestive heart failure in patients treated with doxorubicin. *Cancer* **2003**, *97*, 2869–2879.
- (6) Colabufo, N.; Berardi, F.; Contino, M.; Niso, M.; Perrone, R. ABC pumps and their role in active drug transport. *Curr. Top. Med. Chem.* **2009**, *9*, 119–129.
- (7) Honjo, Y.; Hrycyna, C. A.; Yan, Q. W.; Medina-Pérez, W. Y.; Robey, R. W.; van de Laar, A.; Litman, T.; Dean, M.; Bates, S. E. Acquired mutations in the MXR/BCRP/ABCP gene alter substrate specificity in MXR/BCRP/ABCP-overexpressing cells. *Cancer Res.* **2001**, *61*, 6635–6639.
- (8) Robey, R. W.; Pluchino, K. M.; Hall, M. D.; Fojo, A. T.; Bates, S. E.; Gottesman, M. M. Revisiting the role of ABC transporters in multidrug-resistant cancer. *Nat. Rev. Cancer* **2018**, *18*, 452–464.
- (9) Colabufo, N. A.; Berardi, F.; Cantore, M.; Contino, M.; Inglese, C.; Niso, M.; Perrone, R. Perspectives of P-glycoprotein modulating agents in oncology and neurodegenerative diseases: pharmaceutical, biological and diagnostic potentials. *J. Med. Chem.* **2010**, *53*, 1883–1897.
- (10) Hu, C.-M. J.; Zhang, L. Nanoparticle-based combination therapy toward overcoming drug resistance in cancer. *Biochem. Pharmacol.* **2012**, *83*, 1104–1111.
- (11) Ignarro, L. J. *Nitric Oxide: Biology and Pathobiology*, 2nd ed.; Elsevier Inc., 2010.
- (12) Huang, Z.; Fu, J.; Zhang, Y. Nitric Oxide Donor-Based Cancer Therapy: Advances and Prospects. *J. Med. Chem.* **2017**, *60*, 7617–7635.
- (13) Fukumura, D.; Kashiwagi, S.; Jain, R. K. The role of nitric oxide in tumour progression. *Nat. Rev. Cancer* **2006**, *6*, 521–534.
- (14) Wink, D. A.; Mitchell, J. B. Chemical biology of nitric oxide: insights into regulatory, cytotoxic, and cytoprotective mechanisms of nitric oxide. *Free Radical Biol. Med.* **1998**, *25*, 434–456.
- (15) Moncada, S.; Erusalimsky, J. D. Does nitric oxide modulate mitochondrial energy generation and apoptosis? *Nat. Rev. Mol. Cell Biol.* **2002**, *3*, 214–220.
- (16) Wink, D.; Vodovotz, Y.; Laval, J.; Laval, M. The multifaceted roles of nitric oxide in cancer. *Carcinogenesis* **1998**, *19*, 711–721.
- (17) Riganti, C.; Miraglia, E.; Viarisio, D.; Costamagna, C.; Pescarmona, G.; Ghigo, D.; Bosia, A. Nitric oxide reverts the resistance to doxorubicin in human colon cancer cells by inhibiting the drug efflux. *Cancer Res.* **2005**, *65*, 516–525.
- (18) De Boo, S.; Kopecka, J.; Brusa, D.; Gazzano, E.; Matera, L.; Ghigo, D.; Bosia, A.; Riganti, C. iNOS activity is necessary for the cytotoxic and immunogenic effects of doxorubicin in human colon cancer cells. *Mol. Cancer* **2009**, *8*, 108.

(19) Chegaev, K.; Riganti, C.; Lazzarato, L.; Rolando, B.; Guglielmo, S.; Campia, I.; Fruttero, R.; Bosia, A.; Gasco, A. Nitric oxide donor–doxorubicin conjugates accumulate into doxorubicin resistant human colon cancer cells inducing cytotoxicity. *ACS Med. Chem. Lett.* **2011**, *2*, 494–497.

(20) Riganti, C.; Rolando, B.; Kopecka, J.; Campia, I.; Chegaev, K.; Lazzarato, L.; Federico, A.; Fruttero, R.; Ghigo, D. Mitochondrial-targeting nitrooxy-doxorubicin: a new approach to overcome drug resistance. *Mol. Pharm.* **2013**, *10*, 161–174.

(21) Gazzano, E.; Chegaev, K.; Rolando, B.; Blangetti, M.; Annaratone, L.; Ghigo, D.; Fruttero, R.; Riganti, C. Overcoming multidrug resistance by targeting mitochondria with NO-donating doxorubicins. *Bioorg. Med. Chem.* **2016**, *24*, 967–975.

(22) Sortino, S. Light-controlled nitric oxide delivering molecular assemblies. *Chem. Soc. Rev.* **2010**, *39*, 2903–2913.

(23) Ford, P. C. Photochemical delivery of nitric oxide. *Nitric Oxide* **2013**, *34*, 56–64.

(24) Fry, N. L.; Mascharak, P. K. Photoactive ruthenium nitrosyls as NO donors: how to sensitize them toward visible light. *Acc. Chem. Res.* **2011**, *44*, 289–298.

(25) Ieda, N.; Oka, Y.; Yoshihara, T.; Tobita, S.; Sasamori, T.; Kawaguchi, M.; Nakagawa, H. Structure-efficiency relationship of photoinduced electron transfer-triggered nitric oxide releasers. *Sci. Rep.* **2019**, *9*, 1430–1439.

(26) Chegaev, K.; Fraix, A.; Gazzano, E.; Abd-Ellatef, G. E. F.; Blangetti, M.; Rolando, B.; Conoci, S.; Riganti, C.; Fruttero, R.; Gasco, A.; Sortino, S. Light-regulated NO release as a novel strategy to overcome doxorubicin multidrug resistance. *ACS Med. Chem. Lett.* **2017**, *8*, 361–365.

(27) Fraix, A.; Parisi, C.; Failla, M.; Chegaev, K.; Spyrikis, F.; Lazzarato, L.; Fruttero, R.; Gasco, A.; Sortino, S. NO release regulated by doxorubicin as green light-harvesting antenna. *Chem. Commun.* **2020**, *56*, 6332–6335.

(28) Xu, F.; Wang, F.; Yang, T.; Sheng, Y.; Zhong, T.; Chen, Y. Differential drug resistance acquisition to doxorubicin and paclitaxel in breast cancer cells. *Cancer Cell Int.* **2014**, *14*, 142–154.

(29) Peetla, C.; Bhave, R.; Vijayaraghavalu, S.; Stine, A.; Kooijman, E.; Labhasetwar, V. Drug resistance in breast cancer cells: biophysical characterization of and doxorubicin interactions with membrane lipids. *Mol. Pharm.* **2010**, *7*, 2334–2348.

(30) Hoogenboezem, E. N.; Duvall, C. L. Harnessing albumin as a carrier for cancer therapies. *Adv. Drug Delivery Rev.* **2018**, *130*, 73–89.

(31) Steiner, R. F.; Weinryb, L. *Excited States of Protein and Nucleic Acid*; Plenum Press: New York, 1971; p 40.

(32) Lakowicz, J. R. *Principles of Fluorescence Spectroscopy*, 2nd ed.; Plenum Press: New York, 1999; pp 237–265.

(33) Tayeh, N.; Rungassamy, T.; Albani, J. R. Fluorescence spectral resolution of tryptophan residues in bovine and human serum albumins. *J. Pharm. Biomed. Anal.* **2009**, *50*, 107–116.

(34) Mandeville, J. S.; Tajmir-Riahi, H. A. Complexes of dendrimers with bovine serum albumin. *Biomacromolecules* **2010**, *11*, 465–472.

(35) Agudelo, D.; Bourassa, P.; Bruneau, J.; Bérubé, G.; Asselin, É.; Tajmir-Riahi, H.-A. Probing the binding sites of antibiotic drugs doxorubicin and N-(trifluoroacetyl) doxorubicin with human and bovine serum albumins. *PLoS One* **2012**, *7*, No. e43814.

## Recommended by ACS

### Dual-Targeting and Multimodal Imaging-Guided Photothermal/Chemodynamic Synergistic Therapy Boosted by Ascorbic Acid-Induced H<sub>2</sub>O<sub>2</sub> in Situ Self-Supply

Yang Liu, Peng Jiang, *et al.*

FEBRUARY 09, 2023

ACS APPLIED MATERIALS & INTERFACES

READ 

### A Tumor Microenvironment-Triggered and Photothermal-Enhanced Nanocatalysis Multimodal Therapy Platform for Precise Cancer Therapy

Ling Qiao, Chenxin Cai, *et al.*

NOVEMBER 16, 2021

CHEMISTRY OF MATERIALS

READ 

### Generated Mercury(I) as a Peroxidase-like Activity Modulator via Stimulating the Expression of Active Sites of Silver Nanoparticles for Environmental Hg<sup>2+</sup> Detection

Yingsha Wang, Wenping Hu, *et al.*

JANUARY 21, 2022

ACS APPLIED NANO MATERIALS

READ 

### One-Step Integration of Tumor Microenvironment-Responsive Calcium and Copper Peroxides Nanocomposite for Enhanced Chemodynamic/Ion-Interference Therapy

Bin Liu, Jun Lin, *et al.*

DECEMBER 27, 2021

ACS NANO

READ 